

# Quad-Rotor Directional Steering System Controller Design Using Gravitational Search Optimization

M. A. Kamel<sup>a</sup>, M. A. Abido<sup>b</sup> and Moustafa Elshafei<sup>c</sup>

<sup>a</sup>Systems Engineering Department, King Fahd University of Petroleum and Minerals, Dhahran, Saudi Arabia; <sup>b</sup>Electrical Engineering Department, King Fahd University of Petroleum and Minerals, Dhahran, Saudi Arabia; <sup>c</sup>Department of Mechatronics Engineering, Misr University of Science and Technology, Cairo, Egypt

## ABSTRACT

Directional Steering System (DSS) has been established for well drilling in the oilfield in order to accomplish high reservoir productivity and to improve accessibility of oil reservoirs in complex locations. In this paper, a novel feedback linearization controller to cancel the nonlinear dynamics of a DSS is proposed. The proposed controller design problem is formulated as an optimization problem for optimal settings of the controller feedback gains. Gravitational Search Algorithm (GSA) is developed to search for optimal settings of the proposed controller. The objective function considered is to minimize the tracking error and drilling efforts. In this study, the DSS considered has 4 downhole motors. The robustness of the proposed GSA-based approach for the controller design is demonstrated. The simulation results of the considered 4-rotor DSS is presented and the effectiveness of the proposed controller is confirmed.

## KEYWORDS

Directional drilling; rotary steerable system; quad-rotor; nonlinear control; feedback linearization; gravitational search

## 1. Introduction

Directional Steering System (DSS) has considerable importance in the oil and gas industry due to its influence on the well production rate. It can improve the accessibility of the oil reservoirs beneath difficult to reach locations such as; cities, mountains, and lacks. DSS is crucial if the reservoir is having a wide surface zone in a slim horizontal layer. The horizontal wells can be extended over a larger area in contact with the reservoir providing higher productivity (Talib et al., 2014).

Directional drilling refers to the operation of leading the wellbore along some preplanned trajectory towards a prescribed target. Deviation control is used to keep the wellbore within predetermined limits of inclination angle and/or azimuth angle (Bourgoyne, Chenevert, & Millhelm, 1986). The steering mechanism of directional drilling systems works by applying angular moments and lateral loads to the drill bit in order to modify the propagation direction of the borehole (Downton & Ignova, 2011).

Although the California Huntington Beach field drilled in 1933 is regarded as the first directional oil well, since then different directional drilling techniques have been recently presented. Directional drilling (DD) systems introduced in 1962 had included developments on the positive-displacement-motor and bent-sub-assembly, which made the development of offshore fields practical (Brantly, 1971). This technology was extended and further developed to the concept of steerable motor systems (Garrison, 1965). The development of the steerable motor technology has been improved in its designs and materials (Yiyong et al., 2009). High precision directional drilling technologies have significant importance in extended mineral and seabed resources exploration. They could be considered as a key task of geological work. In order to enhance the precision and quality of geological exploration, a high accuracy DD technique is the

proper option. DD is used to decrease the overall exploration cost and reduce the total drilling platform number, particularly in the maritime resources exploration (Yiyong et al., 2009).

## 2. Related Work

In the last two decades, DD technology has been improved through some oil and gas services companies as Schlumberger, Baker Hughes, and Halliburton amongst others. Other companies that carried out subsequent research in directional systems include Precision Drilling Corporation, Pathfinder, Gyrodata Limited, and Noble Downhole Technology (Chen et al., 2003; Orban & Richardson, 1995; Wu & Wisler, 1993).

Researchers of several companies in China, including China National Offshore Oil Corporation, Xi'an Petroleum Institute, and China Petrochemical Corporation have also investigated the directional drilling system control principle. However, key directionally drilling components, particularly the control unit of the system, has not been fully realized in China (Yiyong et al., 2009).

Directional drilling assembly designs used to drill directional holes are mechanical, hydraulic, electrical, and natural (Haugen, 1998). The techniques used to drill directional holes are rotary drilling with certain stabilizer arrangements (Bobo, 1968), downhole motor with a bent sub (Wenzel, 1988), rotary steerable system (RSS) (Gamer et al., 1992), whipstocks (Frisby, 1967), and jetting drilling (Williams, 1956). All these techniques are classified as mechanical methods except the jetting drilling, which is considered as a hydraulic method. A natural method is related to formation geology such as; hardness and dipping associated with a certain bottom hole assembly (BHA) design. Nowadays, the two most used methods in deep directional drilling are the downhole motor and the RSS.

Rotary steerable systems improve the rate of penetration and extend the reach of extended-reach-drilling (ERD) wells. This increases the efficiency and reduces the total cost of ERD processes. Using those systems, operators can optimize the wellbore placement and hole quality to fulfil a better rate of penetration and improve the reservoir deliverability. RSS were applied for various ERD wells at the Wytch Farm by Colebrook, Peach, Allen, and Conran in 1998 (Colebrook et al., 1998).

A new proposed model of a directional steering system has been developed with different dynamics (Talib et al., 2014), which includes 4 downhole motors where drill bits are attached. The steering mechanism of the proposed quad-motor is comparable to the quad-rotor craft structure. However, designing its control algorithm is more challenging due to the nonlinear coupling in its associated angles, pitch-yaw-roll (Talib et al., 2014). Unlike conventional drilling, the drilling power is mainly coming from these downhole motors. The drill string is not rotating and only transmits the drilling fluid and force on bit.

Conventional directional drilling techniques use deflectors to drive the drill bit laterally through the borehole such as whipstocking (Frisby, 1967). Otherwise, a bent joint can be inserted in the drill-string, i.e. bent subs (Wenzel, 1988). It can also propel pressurized drill mud via a nozzle in the drilling process to drive the bit laterally as side jetting (Williams, 1956). The whipstocking technique demands a sequence of independent processes such as pilot holes punching, reaming of the pilot hole, then remove the deflector. Therefore, the process is costly and needs much more time. The technique of bent subs requires expensive actuators in order to produce lateral forces on the drill bit. The use of side jetting technique is not suitable for all fields such as hard rock earth, because the hard rock will not be eroded by the conventional mud pressure. In addition, this technique uses special drill bits to introduce offset holes by the pressurized drill mud.

The invention reported in (Talib et al., 2014) discloses a drilling apparatus with four drilling motors. The proposed apparatus eliminates the need for the current complicated techniques, and provides simple and intuitive techniques for precise drilling of the desired hole bore trajectory. The rate of rock removal can be precisely controlled by controlling the angular speed of every motor individually. Consequently, the direction of advancement of the drilling head is properly controlled.

Plenty of research studies have been developed in the scope of modeling and optimization of directional drilling. A major part of the reported work aims at minimizing error and cost of the drilling process (Miyora, 2015). Modeling of the drilling operation for control and optimization is a challenging problem due to the diversity of the factors affecting drilling as well as the uncertainty in their determination. Among these factors are the bottom hole assembly (BHA) dynamics, torques and drags, formation properties, bit formation interaction, and drilling fluid properties and its hydraulics (Bourgoyne & Young, 1974).

There are several evolutionary optimization algorithms that are widely used in various applications with impressive success (Chiroma et al., 2016; Xue, Zhong, Ma, & Cao, 2016). Gravitational search algorithm (GSA) for solving the optimization problems has been recently presented (Sabri, Puteh, & Mahmood, 2013). It was reported that the GSA is able to provide more precise, efficient and robust solution for a number of optimization problems. GSA was exercised in different disciplines such as controller design for optimum tuning of PI-fuzzy controllers (David et al., 2012), network routing

(Rubio-Largo et al., 2011), wireless sensor networks (Rostamy, Bernety, & Hosseinabadi, 2011), multi-level thresholding (Sun et al., 2016), renewable micro-grids (Niknam, Golestaneh, & Malekpour, 2012), and PD-fuzzy controller for MIMO systems (Hashim & Abido, 2015). An experimental comparative study has been developed between GSA, central force optimization, particle swarm optimization, and real genetic algorithm (Rashedi, Nezamabadi-pour, & Saryazdi, 2009). It was reported that the results acquired by GSA in most cases are much better compared to other optimization techniques.

Due to its potential, GSA has been hybridized with other evolutionary algorithms and soft computing techniques and the results were impressive. A Fuzzy logic-based adaptive GSA is used for optimal tuning of fuzzy-controlled servo systems (David et al., 2013). The fuzzy controller is used to adapt the gravitational constant and the number of effective agents. The proposed control algorithm showed better performance over other classic control techniques to control the angular speed of a laboratory servo system. In addition, a Modified-GSA is used for feature subset selection in machine learning, (Han et al., 2014). A sequential quadratic programming is used for accelerating local exploitation and the developed algorithm exhibited high performance over other techniques. A Hybrid PSO-GSA algorithm is implemented to improve the power system stability (Khadanga & Satapathy, 2015) where a hybrid algorithm is designed to design the damping controller and overcome time delays and signal transmission delays. The reported results were very adaptive and demonstrated the effectiveness of GSA compared to literature. Another hybridization of GSA with clonal selection algorithm was investigated for global optimization problems (Gao et al., 2013), where GSA was devoted to carry out exploration in the search space while clonal selection algorithm was developed to perform exploitation within the neighbourhood of the found solution. The algorithm showed better performance for eight benchmark functions including both unimodal and multimodal types (Gao et al., 2013).

In this work, the dynamic analysis and control strategy of the quad-rotor directional steering systems are proposed. The proposed strategy aims at designing and controlling the DSS for tracking and stabilization of the drill bit. The proposed control strategy involves linearization of the highly nonlinear dynamics of the system. GSA optimization technique is proposed and developed to optimize the control inputs of the four rotors. The proposed GSA-based optimization procedure overcomes the shortcomings of Linear Quadratic Regulator (LQR) where the weight matrices, Q and R, are subjectively set by trial and error approach. This gives a narrow range for weighting the objective function. In addition, the proposed controller design approach is applicable to wide range of oilfields with unknown formation friction and rock strength as it adaptively estimates the optimal system parameters. The performance of the proposed control strategy are discussed and evaluated.

### 3. Dynamic Analysis

A directional steering mechanism equipped with 4 rotors, as shown in Figure 1, is driving 4 independent bit assemblies. Each rotor speed can be regulated individually, creating a precisely control for the rate of removing rocks by each bit in addition to the progression direction of the drill head. The drilling head assembly is located at the end of the drillstring. The drillstring contains an inner tube for conveying the drilling fluid. The use of four motors in coordination with other

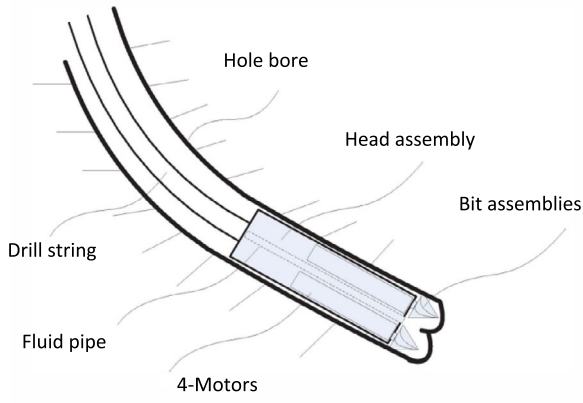


Figure 1. Drilling Head Assembly (Talib et al., 2014).

classical drilling variables permits precise control of the drilling direction and optimization of Rate of Penetration (RoP) (Talib et al., 2014).

Sensors embedded at the head assembly are used to measure the angular orientation of drillstring. This measurement is called measurement-while-drilling (MWD). It inferentially gives the local inclination (i.e. pitch angle) of the borehole. The sensors also indicate the azimuthal direction of the borehole, i.e. the horizontal angular distance from North direction to a point of interest projected on the same plane. Both the azimuthal direction and local inclination are transmitted to a controller, which could be positioned in the drillstring, surface rig, or remote location. This controller takes these measurements as a feedback to identify the current position and shape of the borehole then compare it to the desired borehole trajectory to calculate the steady state error. The controller then computes and transmits a steering direction correction to the DD mechanism (Downton & Ignova, 2011).

The four drill bits are positioned symmetrically with respect to three body axes. The drill bit resolves the motor torque into two main components; a drag torque ( $T_D$ ) on a plane orthogonal to the bit axis, and a lift force ( $F_L$ ), which pushes removed rocks up along the spiral grooves of the drilling bit.

The most commonly used approach for optimization of the actual rotary drilling operation is the mechanical specific energy (MSE). MSE principle is defined as the amount of work desired to crush a certain volume of the rocks. It can be used as an optimization tool during drilling operations where any change in drilling efficiency can be detected in order to enhance instantaneous rate of penetration (RoP) by optimizing the drilling parameters (Rashidi, Hareland, & Nygaard, 2008).

The transformation of the inputs is defined as follows:

$$u_1 = F_{L_1} + F_{L_2} + F_{L_3} + F_{L_4} + FoB \quad (1)$$

$$u_2 = F_{L_2} - F_{L_4} \quad (2)$$

$$u_3 = F_{L_1} - F_{L_3} \quad (3)$$

$$u_4 = T_{D_1} - T_{D_2} + T_{D_3} - T_{D_4} \quad (4)$$

Where:

$u_i$  is the input control action;  $i = 1, 2, 3$  or  $4$ .

$F_{L_i}$  is the motor lift force;  $i = 1, 2, 3$  or  $4$ .

$T_{D_i}$  is the motor drag torque;  $i = 1, 2, 3$  or  $4$ .

$FoB$  stands for Force on Bit, which is a quantitative part used to represent axial force amount placed on the assembly of drill bit. This force directly acts on the center axis of a system. Therefore, it is treated as an additional term of input variable  $u_1$  and usually used to enhance the RoP.

Breaking rocks demands the drag torque ( $T_D$ ) of the actuator to be higher than the lift force ( $F_L$ ). However, higher values of  $F_L$  are required to develop steering and RoP. The  $F_L$  and  $T_D$  are related to the input torque of the motor ( $T_m$ ) and the motor angular speed ( $\omega$ ) by the following expressions,

$$F_{L_i} = \alpha_1 T_{m_i} = b \cdot \omega_i^2 \quad (5)$$

$$T_{D_i} = \alpha_2 T_{m_i} = d \cdot \omega_i^2 \quad (6)$$

Where  $\alpha_1$  and  $\alpha_2$  depend on the geometry of drill bit,  $b$  is the thrust factor that depends on the geometry of drill bit and the density of mud, and  $d$  is the drag factor that depends on the drill bit geometry and rock properties.

Figure 2 illustrates the proposed two fixed frames. Firstly, the earth (inertia) fixed frame referred by E, and, secondly, the body fixed frame denoted B. The orientation of the 4-motor drill bit system is defined by the three Euler angles, namely, roll, pitch, and yaw angles, symbolized as  $\Phi$ ,  $\theta$ , and  $\psi$ , respectively. The proposed dynamic model of the DSS can be represented by the following four nonlinear differential equations:

$$\dot{w} = \frac{1}{m}(u_1 - F_{f_w}) - g \cos \theta \quad (7)$$

$$\ddot{\psi} = \dot{\theta} \dot{\phi} \left( \frac{I_y - I_z}{I_x} \right) - \frac{I_r}{I_x} \dot{\theta} G_u + \frac{L_b u_2}{I_x} \quad (8)$$

$$\ddot{\theta} = \dot{\phi} \dot{\psi} \left( \frac{I_z - I_x}{I_y} \right) + \frac{I_r}{I_y} \dot{\psi} G_u + \frac{L_b u_3}{I_y} \quad (9)$$

$$\ddot{\phi} = \dot{\theta} \dot{\psi} \left( \frac{I_x - I_y}{I_z} \right) + \frac{u_4 - T_{f_w, \psi}}{I_z} \quad (10)$$

Where:

$w$ : measured depth.

$\phi$ ,  $\theta$ , and  $\psi$ : roll, pitch, and yaw angles.

$m$ : mass of the DSS.

$I_x$ ,  $I_y$ , and  $I_z$ : inertia of the DSS.

$I_r$ : inertia of the drill bit.

$g$ : gravitational acceleration.

$F_{f_w}$ : the friction force.

$T_{f_w, \psi}$ : the friction torque.

$G_u$ : gyroscopic torque coefficient.

$T_{f_w}$ ,  $T_{f_w, \psi}$ , and  $G_u$  can be expressed as,

$$F_{f_w} = \mu m g (\sin \theta \cos \phi + \sin \theta \sin \phi) \quad (11)$$

$$T_{f_w, \psi} = \mu r_h m g \cos \theta (\sin \theta \cos \phi + \sin \theta \sin \phi) \quad (12)$$

$$G_u = \omega_1 - \omega_2 + \omega_3 - \omega_4 \quad (13)$$

Where  $\mu$  is the friction coefficient (0.25 ~ 0.4), and  $r_h$  is the hole radius. Equations 1–4 can be rewritten as

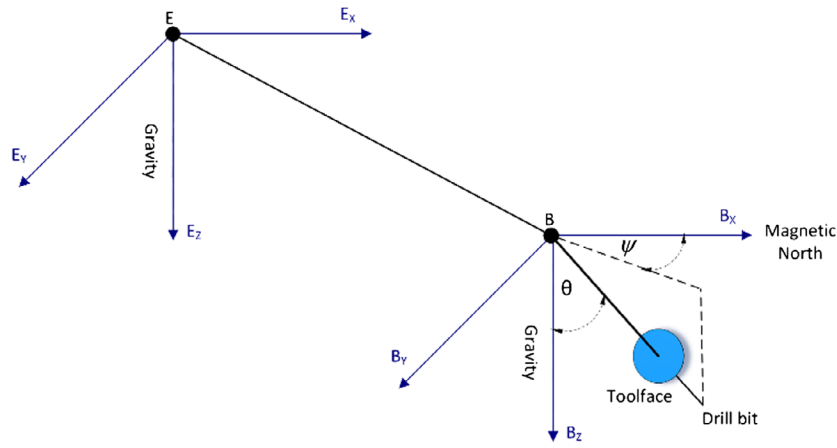


Figure 2. Earth and Body Frame.

$$\begin{bmatrix} u_1 \\ u_2 \\ u_3 \\ u_4 \end{bmatrix} = \begin{bmatrix} b & b & b & b \\ 0 & b & 0 & -b \\ b & 0 & -b & 0 \\ d & -d & d & -d \end{bmatrix} \begin{bmatrix} \omega_1^2 \\ \omega_2^2 \\ \omega_3^2 \\ \omega_4^2 \end{bmatrix} + \begin{bmatrix} 1 \\ 0 \\ 0 \\ 0 \end{bmatrix} \cdot FoB \quad (14)$$

That yields,

$$\begin{bmatrix} \omega_1^2 \\ \omega_2^2 \\ \omega_3^2 \\ \omega_4^2 \end{bmatrix} = \begin{bmatrix} b & b & b & b \\ 0 & b & 0 & -b \\ b & 0 & -b & 0 \\ d & -d & d & -d \end{bmatrix}^{-1} \times \begin{bmatrix} u_1 \\ u_2 \\ u_3 \\ u_4 \end{bmatrix} - \begin{bmatrix} FoB \\ 0 \\ 0 \\ 0 \end{bmatrix} \quad (15)$$

The body axes at any point in the space can be transformed to the earth axes using the transformation matrix R.

$$R = \begin{bmatrix} c\psi c\theta c\phi & -s\psi s\phi & -c\psi c\theta s\phi & -s\psi c\phi & c\psi s\theta \\ s\psi c\theta c\phi & +c\psi s\phi & -s\psi c\theta s\phi & +c\psi c\phi & s\psi s\theta \\ -s\theta c\phi & & s\theta s\phi & & c\theta \end{bmatrix} \quad (16)$$

Where  $s\psi$  and  $c\psi$  denote  $\sin(\psi)$  and  $\cos(\psi)$ , respectively. The location of any point with respect to the earth axes can be formulated as

$$\begin{bmatrix} X_E(t) \\ Y_E(t) \\ Z_E(t) \end{bmatrix} = \begin{bmatrix} X_E(t-1) \\ Y_E(t-1) \\ Z_E(t-1) \end{bmatrix} + R \cdot \begin{bmatrix} 0 \\ 0 \\ 1 \end{bmatrix} \cdot \Delta w(t) \quad (17)$$

Where  $X_E$ ,  $Y_E$ , and  $Z_E$  are the location of any point with respect to the earth axes. The  $\Delta w$  is the change of measured depth and can be calculated as

$$\Delta w(t) = w(t) - w(t-1) \quad (18)$$

Generally, the model structure is illustrated in Figure 3.

#### 4. Proposed Controller Design

The control strategy consists of two control actions. The first step is to linearize the highly nonlinear dynamics of the system using feedback linearization as a nonlinear control approach. Feedback linearization uses the state feedback control to transform the nonlinear system into an equivalent linear system (Khalil, 1996). The second step is to optimize the controller design. In this regard, the gravitational search algorithm is developed and employed, which is an

optimization methodology that inspired by the law of gravity and interactions among masses. In this algorithm, the searcher agents consist of a group of masses that interact with each other depending on the Newtonian gravity and motion laws (Rashedi et al., 2009).

##### 4.1. Feedback Linearization

The system model is highly nonlinear and its complexity is significant. This model can be represented as,

$$\dot{x} = f(x, u, t) \quad (19)$$

Where  $u$  is the vector of control parameters and  $X$  is the vector of the system state variables. Here,  $u$  and  $X$  are defined as

$u = [u_1, u_2, u_3, u_4]$ ,  $u_1 - u_4$  are given in Equations 1–4, respectively.

$$\begin{aligned} X &= [w, \psi, \theta, \phi, \dot{w}, \dot{\psi}, \dot{\theta}, \dot{\phi}] \\ &= [x_1, x_2, x_3, x_4, x_5, x_6, x_7, x_8] \end{aligned} \quad (20)$$

It is worth mentioning that the observed parameters are the states  $x_1, x_2$ , and  $x_3$  that are optimized to track desired values. The final state space equation for the DSS can be written as

$$\dot{X}(t) = \begin{bmatrix} x_5 \\ x_6 \\ x_7 \\ x_8 \\ -g \cos x_3 - \frac{1}{m} F_{fw} + \frac{1}{m} u_1 \\ x_7 x_8 \left( \frac{I_y - I_z}{I_x} \right) - \frac{I_x}{I_x} x_7 G_u + \frac{I_b}{I_x} u_2 \\ x_6 x_8 \left( \frac{I_z - I_x}{I_y} \right) + \frac{I_x}{I_y} x_6 G_u + \frac{I_b}{I_y} u_3 \\ x_6 x_7 \left( \frac{I_x - I_y}{I_z} \right) - \frac{T_{fw}}{I_z} + \frac{u_4}{I_z} \end{bmatrix} \quad (21)$$

It can be remarked from the system model equations that the system is fully actuated and has minimum phase dynamics. The system dynamics can be linearized with respect to the control  $u$  using

$$u_1 = m \left( g \cos x_3 + \frac{1}{m} F_{fw} + v_1 \right) \quad (22)$$

$$u_2 = \frac{I_x}{L_b} \left( \frac{I_r}{I_x} x_7 G_u - x_7 x_8 \frac{I_y - I_z}{I_x} + v_2 \right) \quad (23)$$

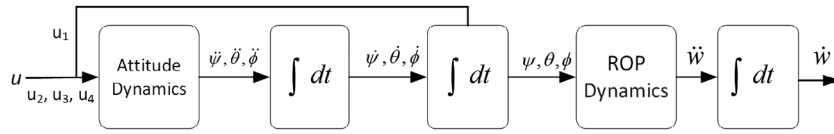


Figure 3. Structure of a DSS Model.

$$u_3 = \frac{I_y}{L_b} \left( -\frac{I_r}{I_y} x_6 G_u - x_6 x_8 \frac{I_z - I_x}{I_y} + v_3 \right) \quad (24)$$

$$u_4 = I_z \cdot \left( -x_6 x_7 \frac{I_x - I_y}{I_z} + v_4 \right) + T_{fw,\psi} \quad (25)$$

Where  $v_i$ ,  $i = 1, 2, 3, 4$  is the new control signals that help to implement the desired operation.

$$v_i = K_i (x_a - x_d); i = 1, 2, 3, \text{ and } 4 \quad (26)$$

$K$  is the feedback gain,  $x_a$  is the actual value of a variable and  $x_d$  is its desired value. The feedback loop depends on the MWD. These drilling apparatuses continuously and automatically provide real-time reading of drilling parameters such as the orientation and the location of the bottom-hole-assembly (BHA) and then send acquired data to the main computer in order to display, record, print, and provide the control action (Chen, Yanshun, & Chunyu, 2010).

The controllability canonical form for the linearized model can be rewritten as

$$\dot{X} = \begin{bmatrix} 0 & 0 & 0 & 0 & 1 & 0 & 0 & 0 \\ 0 & 0 & 0 & 0 & 0 & 1 & 0 & 0 \\ 0 & 0 & 0 & 0 & 0 & 0 & 1 & 0 \\ 0 & 0 & 0 & 0 & 0 & 0 & 0 & 1 \\ 0 & 0 & 0 & 0 & 0 & 0 & 0 & 0 \\ 0 & 0 & 0 & 0 & 0 & 0 & 0 & 0 \\ 0 & 0 & 0 & 0 & 0 & 0 & 0 & 0 \\ 0 & 0 & 0 & 0 & 0 & 0 & 0 & 0 \end{bmatrix} \begin{bmatrix} x_1 \\ x_2 \\ x_3 \\ x_4 \\ x_5 \\ x_6 \\ x_7 \\ x_8 \end{bmatrix} + \begin{bmatrix} 0 & 0 & 0 & 0 \\ 0 & 0 & 0 & 0 \\ 0 & 0 & 0 & 0 \\ 0 & 0 & 0 & 0 \\ 1 & 0 & 0 & 0 \\ 0 & 1 & 0 & 0 \\ 0 & 0 & 1 & 0 \\ 0 & 0 & 0 & 1 \end{bmatrix} \begin{bmatrix} v_1 \\ v_2 \\ v_3 \\ v_4 \end{bmatrix} \quad (27)$$

The cost (objective) function  $J_1$  for tracking a predefined trajectory is formulated as

$$J_1 = \frac{1}{2} [(X_1(k+1) - X_d(k+1))^T Q (X_1(k+1) - X_d(k+1)) + V(k)^T R V(k)] \quad (28)$$

Where  $X_d$  is the desired well trajectory vector including the measured depth, azimuth and inclination angles,  $X_1$  is the model states vector,  $V$  is the vector of new control inputs,  $k$  is the distance step, and  $Q$  &  $R$  are weighting matrices. In this study,  $Q$  is given more weight to minimize the tracking error.

$$X_1 = \begin{bmatrix} w & \psi & \theta \end{bmatrix}^T \quad (29)$$

$$X_d = \begin{bmatrix} w_d & \psi_d & \theta_d \end{bmatrix}^T \quad (30)$$

$$V = \begin{bmatrix} v_1 & v_2 & v_3 & v_4 \end{bmatrix}^T \quad (31)$$

The objective of the optimization techniques is to select the proper feedback gains  $K$ s to optimize the control input signals that leads the system to satisfy the physical restrictions in addition to maximize (or minimize) some performance criterion (Kirk, 1998).

In aerial vehicles applications the values of thrust factor  $b$  and drag factor  $d$  may be considered as constants (Voos, 2009). However, in oilfield drilling, these factors change continuously as going deeper. Therefore,  $b$  and  $d$  have to be optimized at each iteration using an optimization technique to improve the dynamic model accuracy as shown in Figure 4.

Where  $e_1$  and  $e_2$  are defined as

$$e_1 = X_d - X \quad (32)$$

$$e_2 = X_s - X \quad (33)$$

It is worth mentioning that  $e_1$  is used for optimizing the feedback gains while  $e_2$  is used for optimizing the thrust and drag factors.

The estimation accuracy of factors  $b$  and  $d$  depends on the minimization of  $e_2$ . So, the objective function for estimating  $b$  and  $d$  is formulated as

$$J_2 = \frac{1}{2} [(X(k) - X_s(k))^T Q (X(k) - X_s(k))] \quad (34)$$

Where  $X$  is the model states vector and  $X_s$  is the simulator states vector that can be defined as follows:

$$X_s = [w_s, \psi_s, \theta_s, \phi_s, \dot{w}_s, \dot{\psi}_s, \dot{\theta}_s, \dot{\phi}_s] \quad (35)$$

Since the optimization problem formulated has a high dimensional search domain, the conventional optimization techniques have limited capability as the search domain grows exponentially with the size of the problem (Rashedi et al., 2009). Over the past few decades, there was an increasing interest in techniques inspired by the physical processes and biological behavior (Dorigo, Maniezzo, & Colorni, 1996; Farmer, Packard, & Perelson, 1986; Kennedy & Eberhart, 1995; Kim, Abraham, & Cho, 2007; Kirkpatrick, Gelatt, & Vecchi, 1983). It was demonstrated by many researchers that these algorithms are proper for solving complicated computational problems. These include dynamic optimization (Du & Li, 2008), pattern recognition (Tan & Bhanu, 2006), controller design (Baojiang & Shiyong, 2007; Hashim, El-Ferik, & Abido, 2015), and image processing (Cordón, Damas, & Santamaría, 2006; Nezamabadi-pour, Saryazdi, & Rashedi, 2006).

#### 4.2. Gravitational Search Algorithm

Gravitation is defined in physics as the trend of two masses to move towards each other as shown in Figure 5. In this figure,

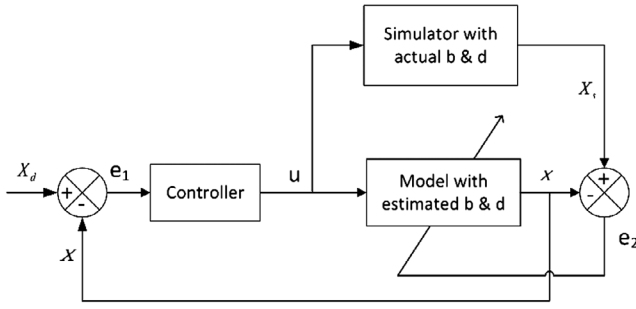


Figure 4. Overall Control Strategy of the Quad-rotor DSS.

$M_1, M_2, M_3,$  and  $M_4$  are four masses with different weights.  $F_{12}, F_{13},$  and  $F_{14}$  are the gravitational forces applied from  $M_1$  towards  $M_2, M_3,$  and  $M_4,$  respectively.  $F_1$  is the equivalent attraction force of  $F_{12}, F_{13},$  and  $F_{14}.$  Here,  $a_1$  is the generated acceleration of  $M_1.$  In the gravitational law of Newton, each mass (body) attracts the other masses with a force, which is called the gravitational force (Rafsanjani & Dowlatshahi, 2012). This force is directly proportional to the product of their masses ( $M_1$  and  $M_2$ ) and inversely proportional to the square of the distance  $R$  between them.

The gravitational force,  $F,$  is expressed as

$$F = C_g \frac{M_1 M_2}{R^2} \quad (36)$$

$C_g$  is the gravitational constant. The general steps of the gravitational search algorithm can be summarized as

**Step 1 (Initialization):** Initialize the iteration counter with  $t = 0$  then create arbitrarily  $n$  agents,  $\{P_j(0), j = 1, 2, \dots, n\},$  where  $P_j(0) = [p_{j,1}(0), p_{j,2}(0), \dots, p_{j,m}(0)]$  where  $m$  is the number of the optimized parameters.  $p_{j,d}(0)$  is created randomly by selecting a value within the  $d$ th optimized parameter range  $[p_d^{\min}, p_d^{\max}]$  using uniform distribution. Evaluate the fitness using the cost function then calculate the best and worst values.

**Step 2 (Iteration updating):** Update the iteration counter  $t = t + 1.$

**Step 3 (Gravitational constant updating):** The gravitational constant ( $C_g$ ) is initialized at  $t = 0$  and decreased with iterations to improve the exploration accuracy,  $C_g(t) = f(C_{g,0}, t)$  where  $C_{g,0}$  is the initial value. The value of  $C_g$  is expressed as

$$C_g(t) = C_{g,0} \times e^{-\alpha(t/t_{\max})} \quad (37)$$

Where  $t_{\max}$  is the maximum number of iterations and  $\alpha$  is a positive integer.

**Step 4 (Acceleration updating):** Using the law of motion, the acceleration of the agent  $j$  at iteration  $t$  is calculated according to the below equations:

$$a_{j,d}(t) = \frac{F_{j,d}(t)}{M_{jj}(t)} \quad (38)$$

$$F_{j,d}(t) = \sum_{k=1, k \neq j}^n rand_k F_{jk,d}(t) \quad (39)$$

Where  $M_{jj}$  is the inertial mass of  $j$ th agent and  $F_{j,d}$  is the total force acting on agent  $j$  in dimension  $d,$   $rand_k$  is a random number in the interval  $[0,1],$  and  $F_{jk}$  is the force acting on agent (mass)  $j$  from mass  $k.$  Those forces are multiplied by a random

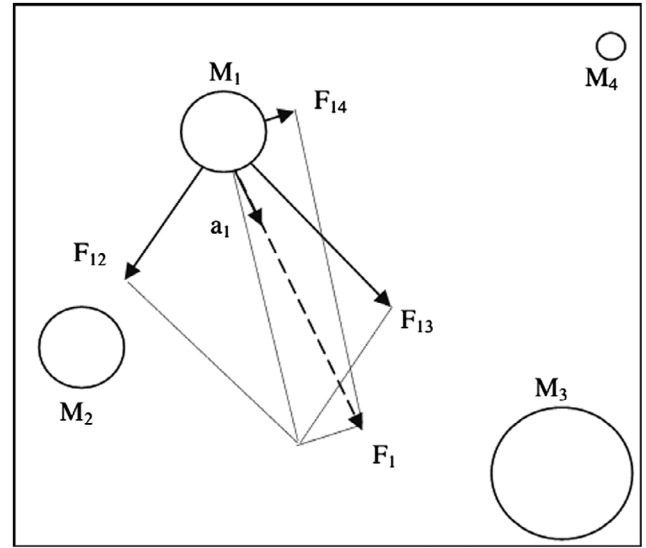


Figure 5. The Acceleration of each Mass Towards the Resultant Force Acting from every other Masses.

number to give a stochastic characteristic to the algorithm.  $F_{jk}$  in the  $d$ th dimension can be calculated as follows:

$$F_{jk,d}(t) = C_g(t) \frac{M_{pj}(t) \times M_{ak}(t)}{R_{jk}(t) + \varepsilon} (p_{k,d}(t) - p_{j,d}(t)) \quad (40)$$

Where  $M_{ak}$  is the active gravitational mass for agent  $k,$   $M_{pj}$  is the passive gravitational mass for agent  $j,$   $C_g(t)$  is the gravitational constant at iteration  $t,$   $\varepsilon$  is a small constant, and  $R_{jk}(t)$  is the Euclidian distance between two agents  $j$  and  $k$  at iteration  $t.$  Those parameters can be calculated as follows:

$$R_{jk}(t) = \left\| P_j(t), P_k(t) \right\|_2 \quad (41)$$

$$M_{aj} = M_{pk} = M_{jj} = M_j, \quad j = 1, 2, \dots, n \quad (42)$$

$$m_j(t) = \frac{fit_j(t) - worst(t)}{best(t) - worst(t)} \quad (43)$$

$$M_j(t) = \frac{m_j(t)}{\sum_{j=1}^n m_k(t)} \quad (44)$$

**Step 5 (Velocity updating):** Update the velocity of the  $j$ th agent in the  $d$ th dimension depending on the updated acceleration using the below equation

$$s_{j,d}(t+1) = rand_j \times s_{j,d}(t) + a_{j,d}(t) \quad (45)$$

**Step 6 (Position updating):** Update the position of the  $j$ th agent in the  $d$ th dimension according to the updated velocity as follows:

$$p_j(t+1) = p_{j,d}(t) + s_{j,d}(t+1) \quad (46)$$

**Step 7 (Fitness updating):** Calculate the fitness of the updated parameters then search for the new best and worst values.

**Step 8 (Stopping criteria):** If the pre-specified number of generations or any other stopping criteria is reached then stop, else go back to step 2.

The above steps are illustrated in the computational flow-chart of GSA as shown in Figure 6.

### 4.3. Controller Design

The proposed control system begins with linearizing the non-linear dynamic system in Equation (21) using the system inputs to facilitate the tracking problem. Then, the controller gains in Equation (26) should be optimized to improve the system response using GSA. Finally, to make the control system act adaptively to overcome any changes in the operation conditions or parameters, the GSA is applied to estimate the actual values of the system parameters  $b$  and  $d$ , based on obtained data from previous iterations as given in Equations (5) and (6). The flow-chart of the overall control algorithm of the quad-rotor DSS is shown in Figure 7.

For the given two minimization problems, the feedback gains represent the agents to minimize the first objective function (fitness) and can be formulated as

$$\begin{aligned} & \underset{K_s}{\text{Minimize}} \quad J_1 \\ & \text{Subject to} \quad 0 \leq K_i \leq 5 \quad i = 1, \dots, 8 \end{aligned} \quad (47)$$

Factors  $b$  &  $d$  represent the agents of the second minimization problem in order to minimize the second objective function (fitness) and can be formulated as

$$\begin{aligned} & \underset{b,d}{\text{Minimize}} \quad J_2 \\ & \text{Subject to} \quad 1 \leq b, d \leq 100 \end{aligned} \quad (48)$$

### 5. Results and Discussions

An iterative simulation mechanism has been implemented to validate the proposed optimization approach with feedback linearization controller. The proposed model for DSS is simulated using Matlab with the given parameters of Table 1. Firstly, the linearized system dynamics in Equation (27) is solved at each iteration with given initial conditions. Secondly, the developed GSA has been applied at each iteration to search for the optimal gains to optimize the control input action in order to improve the system performance and minimize the error from the pre-planned trajectory. Lastly, the developed GSA has been used to estimate the exact values of system parameters  $b$  and  $d$ . The parameters setting for the GSA is given in Table 2.

The optimization algorithm has been applied for two different well trajectories from the Middle East with zero initial  $X_E$ ,  $Y_E$ , and  $Z_E$ . The following simulation results were obtained for the measured depth as shown in Figure 8 and Figure 9 for well-1 and well-2, respectively. A 3D plot of the trajectory tracking is presented in Figure 10 and Figure 11 for well-1 and well-2, respectively. The mean square error between simulator

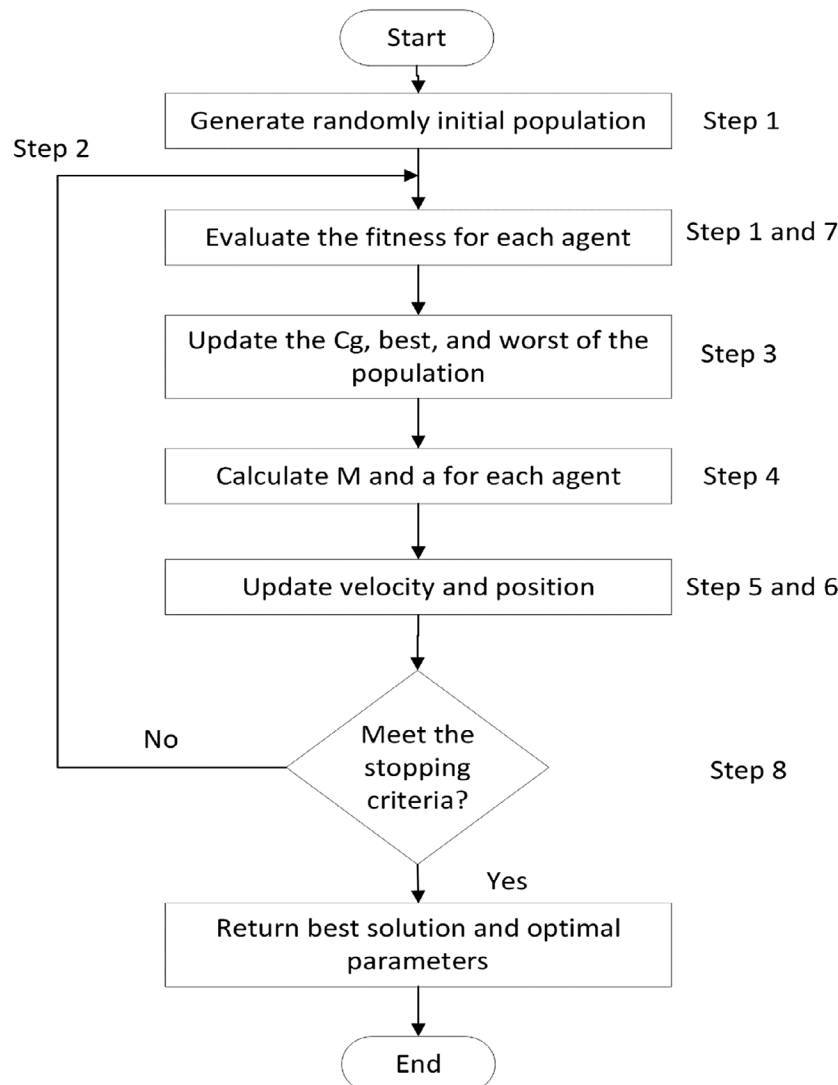


Figure 6. Gravitational Search Algorithm.

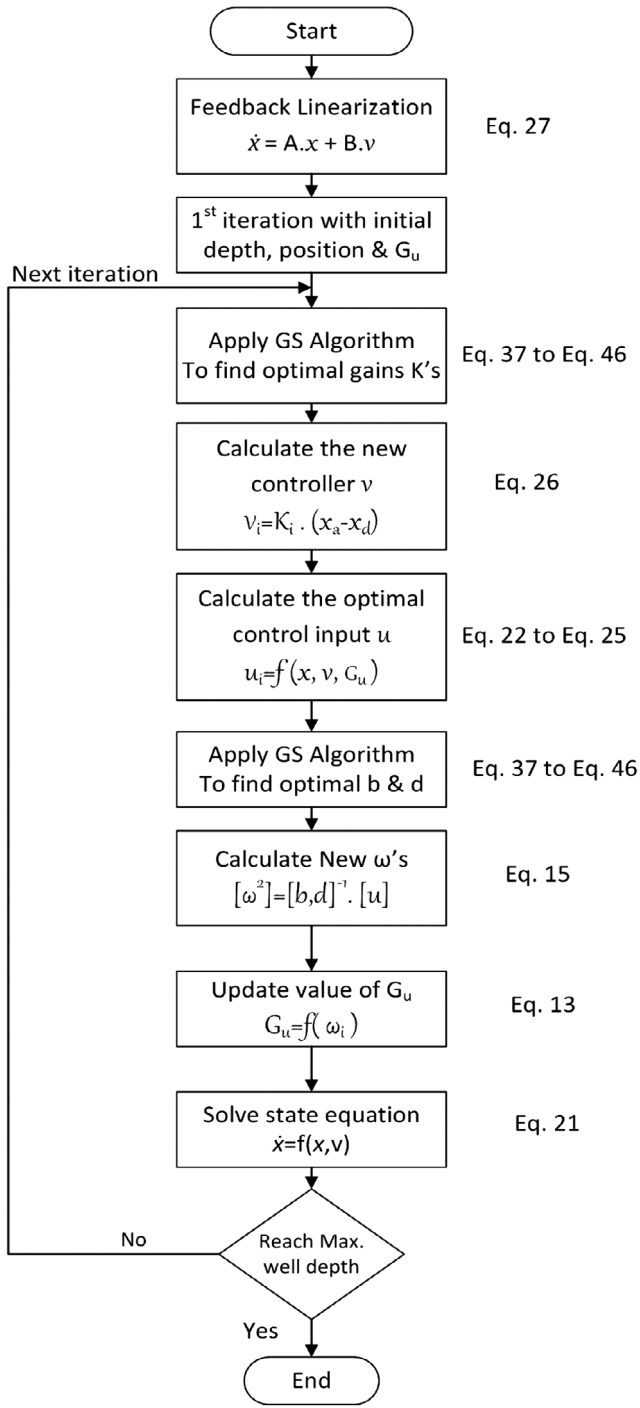


Figure 7. Overall Control Algorithm of Quad-rotor DSS.

Table 1. DSS Dynamic Parameters.

Parameter	Value	Unit
$g$	9.81	$m/s^2$
$m$	200	kg
$L_b$	0.55	m
$I_x = I_y$	60	$kg/m^2$
$I_z$	25	$kg/m^2$
$I_r$	0.83	$kg/m^2$
$\mu$	0.3	-

Table 2. Parameters Setting for GSA.

Parameter	$\alpha$	$\epsilon$	$C_g$	# Pop.	# iter.
Setting	7	0.00001	100	50	100

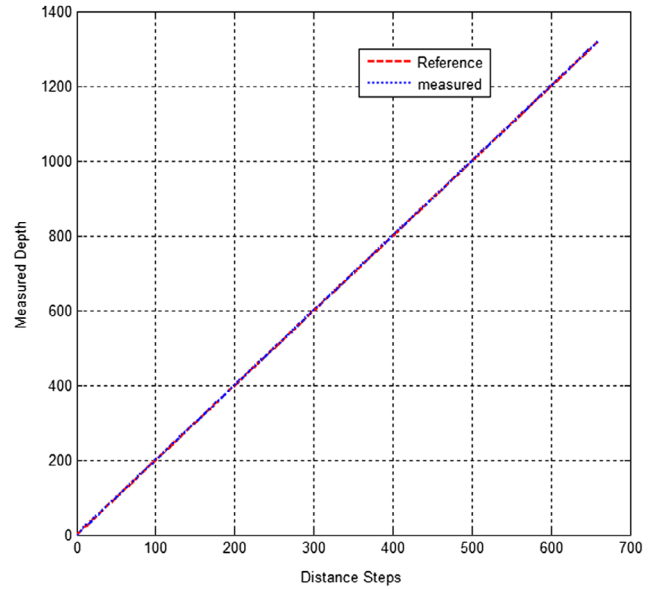


Figure 8. The Response of Measured Depth of Well-1.

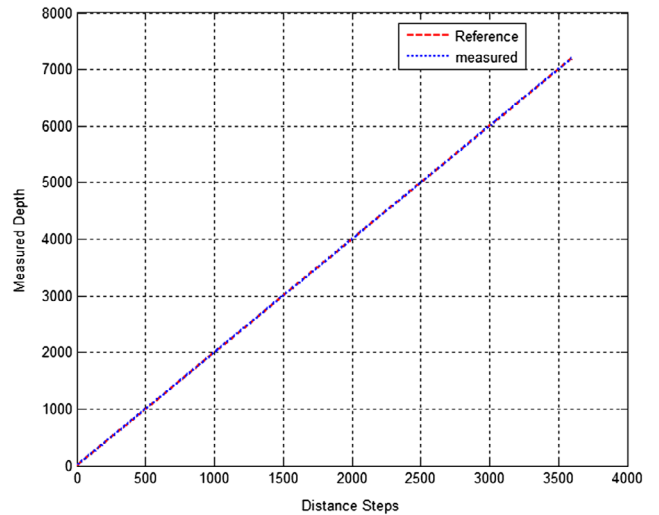


Figure 9. The Response of Measured Depth of Well-2.

and model states is illustrated in Figure 12 and Figure 13 for well-1 and well-2, respectively.

It can be seen that the value of the measured depth is identical to the trajectory of both wells as shown in Figure 8 and Figure 9. In Figure 10 and Figure 11, values of North, East, and True Vertical Depth (TVD) represent the earth coordinates that can be calculated using Equation 17. The root mean square values of the Euclidian distance between the desired trajectory and the actual path of well-1 and well-2 using the proposed optimized GSA-based control strategy are 3.32 meters and 1.99 meters, respectively. On the other hand, the root means square errors of well-1 and well-2 using LQR presented in Talib et al. (2014) are 4.19 meters and 2.82 meters, respectively. It can be concluded that the proposed GSA-based control strategy reduces the trajectory error by 20.8% and 29.4% for well-1 and well-2, respectively compared to LQR (Talib et al., 2014). The obtained results clearly confirm the high performance and superiority of the proposed GSA control strategy. The results also demonstrate the robustness and effectiveness of the proposed control strategy over a wide range of operating conditions.

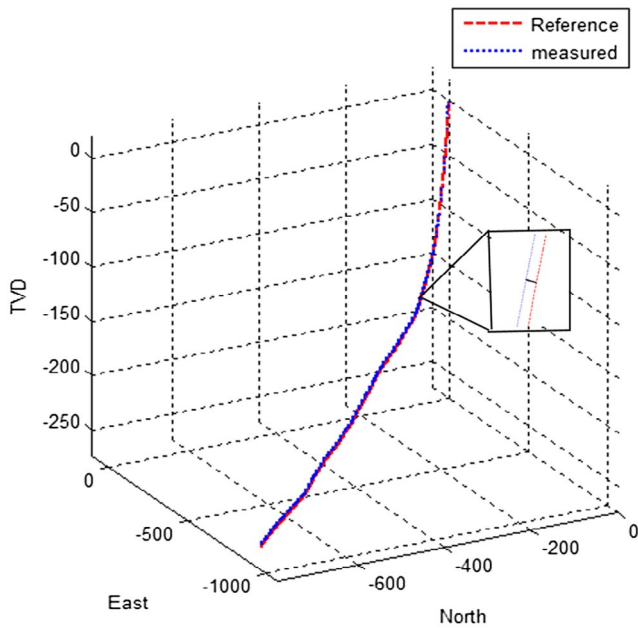


Figure 10. 3D Plot of the Trajectory Tracking of Well-1.

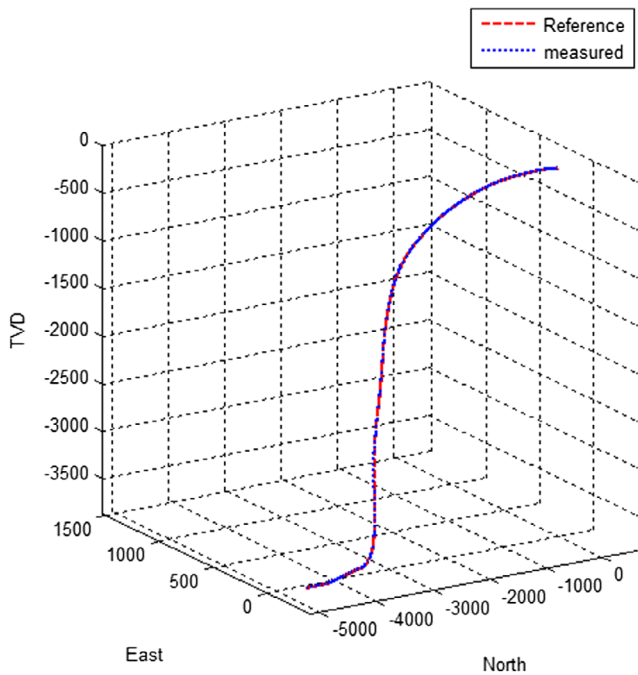


Figure 11. 3D Plot of the Trajectory Tracking of Well-2.

The value of mean square error represented in Figure 12 and Figure 13 measures the accuracy of estimation for the values of thrust factor  $b$  and drag factor  $d$ . These figures show the difference between the simulator states including real values of  $b$  and  $d$  and the model states with the estimated values. The root mean square value of well-1 is 0.0091 while the maximum value for the same well is 0.105 due to a suddenly change in the formation. Additionally, the root mean square value of well-2 is 0.0016 while the maximum value for the same well is 0.06.

In order to demonstrate the robustness and evaluate its performance, the developed GSA approach for optimal controller design has been executed several times with different settings and initial populations. The response of the fitness function minimization versus iterations with different parameters settings is shown in Figure 14. The fitness value is gradually

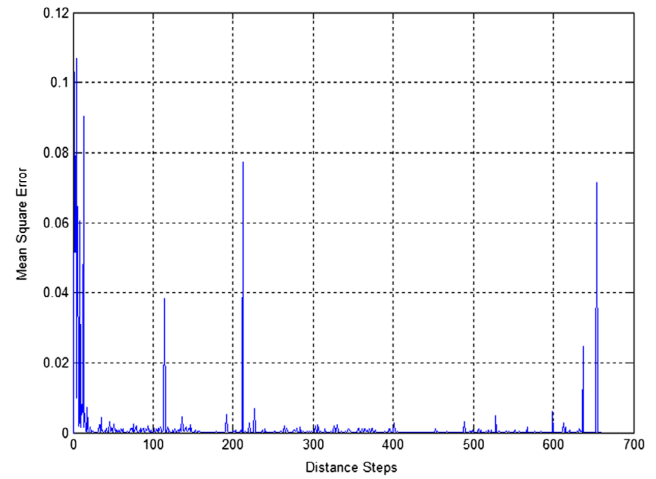


Figure 12. Mean Square Error between Simulator and Model States of Well-1.

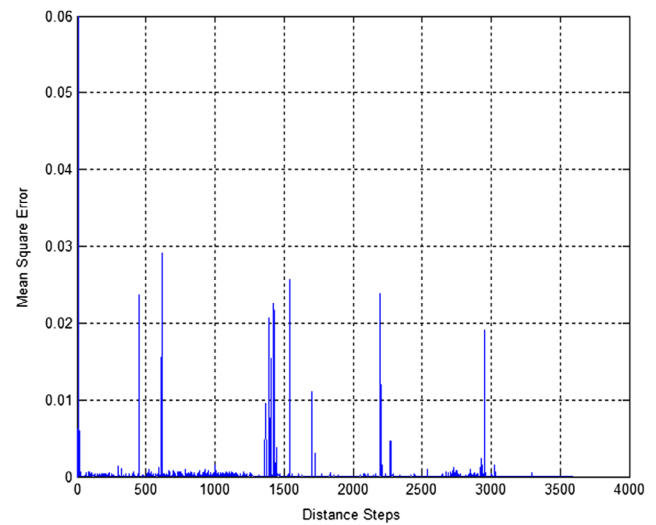
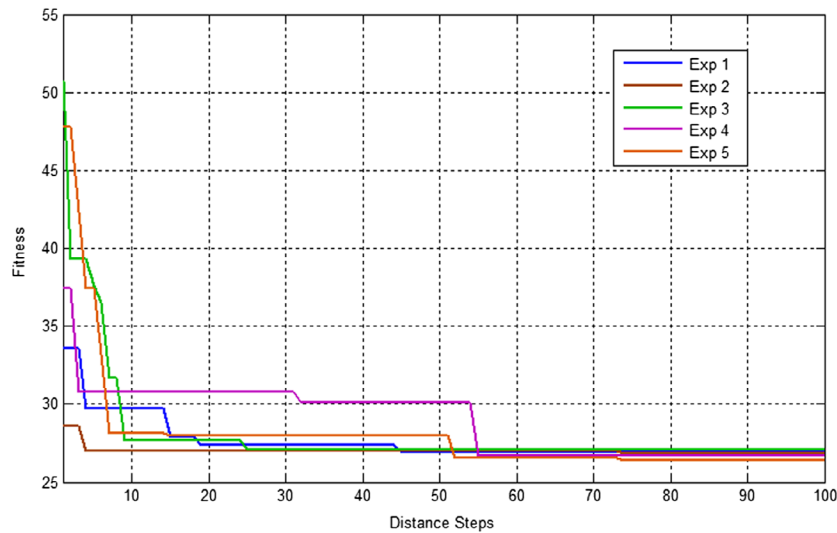


Figure 13. Mean Square Error between Simulator and Model States of Well-2.

decreasing to a suitable value, which is reflected on the output performance. Table 3 presents the five experiments with different initial gravitational constant value  $C_g$  and the constant  $\alpha$ . It can be seen that the best and worst experiments have a fitness function of 26.38 and 27.04, respectively, with an average of 26.76. The closeness of these values confirms the robustness of the developed GSA with respect to its setting and initialization.

## 6. Conclusion

In this work, a new control strategy for the quad-rotor directional steering system is proposed and implemented. The controller design has been formulated as an optimization problem. The gravitational search algorithm has been developed and implemented. Two stages of optimization are proposed in this work to search for the optimal gains of the feedback linearization controller and estimate system parameters  $b$ , and  $d$  in order to enhance the tracking capability. The effectiveness of the proposed controller has been evaluated using two different wells. The results show an improved response of the root mean square value of the Euclidian distance between the desired trajectory and the actual path for two wells considered with the proposed optimized gravitational search algorithm based control strategy. The superiority of the proposed controller



**Figure 14.** Fitness Function Minimization with GSA with Different Parameter Settings.

**Table 3.** Fitness Values for Five Experiments.

	$C_g$	$a$	Fitness Min
Exp 1	100	7	26.9
Exp 2	90	7	26.85
Exp 3	80	7	27.04
Exp 4	100	6	26.67
Exp 5	100	8	26.38

performance has been demonstrated through a comparison with LQR reported in literature. In addition, the robustness of the proposed design approach has been confirmed through several runs. It can be concluded that the proposed control system provides more flexible steering mechanism where each rotor can be controlled individually with non-rotating drillstring. In addition, The results demonstrate that the proposed controller can be applied in wide range of oilfields with unknown formation friction and rock strength.

## Acknowledgement

The authors would like to acknowledge the support provided by King Abdulaziz City for Science and Technology (KACST) through the Science and Technology Unit at King Fahd University of Petroleum and Minerals (KFUPM) for funding this work through project No. 12-OIL3033-04 and project No. 14-ENE265-04 as a part of the National Science, Technology and Innovation Plan (NSTIP).

## Disclosure statement

No potential conflict of interest was reported by the authors.

## Notes on contributors



**Mahmoud A. Kamel** Obtained M.Sc. in Systems and Control Engineering from KFUPM in 2016, with a background in Mechatronics, Robotics, and Control. He gained B.Sc. in Mechatronics Engineering from Helwan University Cairo, Egypt. He has 6 years of experience in research and academia and has several international research papers and conferences.



**M. A. Abido** Currently is a Distinguished University professor at KFUPM. Dr. Abido is the recipient of KFUPM *Excellence in Research Award*, 2002, 2007 and 2012, KFUPM *Best Project Award*, 2007 and 2010, *First Prize Paper Award* of the Industrial Automation and Control Committee of the IEEE Industry Applications Society, 2003, *Abdel-Hamid Shoman Prize for Young Arab Researchers in Engineering Sciences*, 2005.



**Moustafa Elshafei** Is a professor in the of Control and Instrumentation Systems Engineering Department, and obtained a Ph.D. in Electrical Engineering from McGill in 1982 (Dean List), Canada. Since then he has accumulated over 24 years of academic experience and 9 years of industrial experience. He is inventor/co-inventor of 20 USA and international patents, Author/Co-author of 5 books, and published over 170 articles in international journals and professional conferences in the fields of intelligent instrumentation, digital signal processing, artificial intelligence, and industrial control/ automation systems. Dr. Elshafei has been involved in many projects at KFUPM, supported by KFUPM, Saudi ARAMACO, SABIC, YOKOGAWA, KACST, Department of Civil Defense, and NSTIP.

## References

- Baojiang, Z., & Shiyong, L. (2007). Ant colony optimization algorithm and its application to Neuro-Fuzzy controller design. *Journal of Systems Engineering and Electronics*, 18, 603–610.
- Bobo, R.A. (1968). Drill string stabilizer. *US Patent US3419094*. Houston, Texas: Reed Roller Bit Company.
- Bourgoyne, A.T., & Young, F.S., Jr (1974). A multiple regression approach to optimal drilling and abnormal pressure detection. *Society of Petroleum Engineers Journal*, 14, 371–384.
- Bourgoyne, A.D., Chenevert, M.E., Millhelm, K.K., Y.F.S. (1986). Applied drilling engineering. *Society of Petroleum Engineers*, 2, 351–453.
- Brantly, J.E. (1971). *History of oil well drilling*, by Brantly. Houston: Gulf Publishing Company.
- Chen, C.K.D., Gaynor, T.M., Gleitman, D.D., Hardin, J.R., Walker, C., Rao, M.V., & Boulton, R. (2003). Steerable drilling system and method. *US Patents US6581699*. Texas: Halliburton Energy Services Inc.
- Chen, C., Yanshun, Z., & Chunyu, L. (2010). Surveying method of measurement while drilling based on the inertial sensor. *2010 First International Conference on Pervasive Computing, Signal Processing and Applications*, 17–19 September, Harbin, China, (pp. 1192–1195).

- Chiroma, H., Abdul-kareem, S., Shukri Mohd Noor, A., Abubakar, A.I., Sohrabi Safa, N., Shuib, L., ... Fatihu Hamza, M. (2016). A review on artificial intelligence methodologies for the forecasting of crude oil price. *Intelligent Automation & Soft Computing*, 22, 449–462.
- Colebrook, M.A., Peach, S.R., Allen, F.M., Exploration, B.P., Conran, G., & Schlumberger, A. (1998). Application of Steerable Rotary Drilling Technology to Drill Extended Reach Wells. *IADC/SPE Drilling Conference*. 3–6 March, Dallas, Texas. 1–11
- Cordón, O., Damas, S., & Santamaría, J. (2006). A fast and accurate approach for 3D image registration using the scatter search evolutionary algorithm. *Pattern Recognition Letters*, 27, 1191–1200.
- David, R.-C., Precup, R., Petriu, E.M., Purcaru, C., & Preitl, S. (2012). PSO and GSA algorithms for fuzzy controller tuning with reduced process small time constant sensitivity. *16th International Conference on System Theory, Control and Computing (ICSTCC)*, 12–14 Oct., Sinaia, Romania, pp. 1–6.
- David, R.E., Precup, R.C., Radac, M.-B., Preitl, S., & Petriu, E.M. (2013). Fuzzy logic-based adaptive gravitational search algorithm for optimal tuning of fuzzy-controlled servo systems. *IET Control Theory & Applications*, 7, 99–107.
- Dorigo, M., Maniezzo, V., & Colomi, A. (1996). Ant system: Optimization by a colony of cooperating agents. *IEEE Transactions on Systems, Man and Cybernetics, Part B (Cybernetics)*, 26, 29–41.
- Downton, G., & Ignova, M. (2011). Stability and response of closed loop directional drilling system using linear delay differential equations. *Control Applications (CCA)*, IEEE International Conference on Control Applications (CCA), Denver, CO, 28–30 Sept., pp. 893–898.
- Du, W., & Li, B. (2008). Multi-strategy ensemble particle swarm optimization for dynamic optimization. *Information Sciences*, 178, 3096–3109.
- Farmer, J.D., Packard, N.H., & Perelson, A.S. (1986). The immune system, adaptation, and machine learning. *Physica D: Nonlinear Phenomena*, 22, 187–204.
- Frisby, T.M. (1967). Whipstocks. *US Patent US3339636*, Denver: Eastman Oil Well Survey Co. 1–5.
- Gamer, E.F., Hueneme, P., Beach, R., & Nelson, P.E.A. (1992). Actively controlled rotary steerable system and method for drilling wells. *US Patent US6092610*, Schlumberger Technology Corporation.
- Gao, S., Chai, H., Chen, B., & Yang, G. (2013). Hybrid gravitational search and clonal selection algorithm for global optimization. In D. Hutchison, T. Kanade, & J. Kittler (Eds.), *Advances in Swarm Intelligence: 4th International Conference, ICSI 2013, Harbin, China, June 12–15, 2013, Proceedings, Part II* (pp. 1–10). Berlin, Heidelberg: Springer, Berlin Heidelberg.
- Garrison, E.P. (1965). Downhole motor cuts directional drilling costs. *Petroleum Engineer*, January.
- Han, X., Chang, X., Quan, L., Xiong, X., Li, J., Zhang, Z., & Liu, Y. (2014). Feature subset selection by gravitational search algorithm optimization. *Information Sciences*, 281, 128–146.
- Hashim, H.A., & Abido, M.A. (2015). Fuzzy controller design using evolutionary techniques for twin rotor MIMO system: A comparative study. *Intell. Neuroscience*, 2015, 49:49–49:49, 1–11.
- Hashim, H.A., El-Ferik, S., & Abido, M.A. (2015). A fuzzy logic feedback filter design tuned with PSO for L1 adaptive controller. *Expert Systems with Applications*, 42, 9077–9085.
- Haugen, J. (1998). Rotary steerable system replaces slide mode for directional drilling applications. *Oil and Gas Journal*, 45, 1471.
- Kennedy, J., & Eberhart, R. (1995). Particle swarm optimization. *Neural Networks, 1995. Proceedings., IEEE International Conference on*, 4, 1942–1948.
- Khadanga, R.K., & Satapathy, J.K. (2015). Time delay approach for PSS and SSSC based coordinated controller design using hybrid PSO–GSA algorithm. *International Journal of Electrical Power & Energy Systems*, 71, 262–273.
- Khalil, H.K. (1996). *Nonlinear systems* (2nd ed.). Upper Saddle River: Prentice Hall.
- Kim, D.H., Abraham, A., & Cho, J.H. (2007). A hybrid genetic algorithm and bacterial foraging approach for global optimization. *Information Sciences*, 177, 3918–3937.
- Kirk, D.E. (1998). *Optimal Control Theory*. Mineola, New York: Dover Publications.
- Kirkpatrick, S., Gelatt, C.D., & Vecchi, M.P. (1983). Optimization by simulated annealing. *Science*, 220, 671–680.
- Miyora, T.O. (2015, January 26–28). Modelling and optimization of geothermal drilling parameters - A case study of well Mw-17 in Menengai, Kenya. *Fourtieth Workshop on Geothermal Reservoir Engineering Stanford University* (pp. 1–15). Stanford, California, (Figure 4).
- Nezamabadi-pour, H., Saryazdi, S., & Rashedi, E. (2006). Edge detection using ant algorithms. *Soft Computing*, 10, 623–628.
- Niknam, T., Golestaneh, F., & Malekpour, A. (2012). Probabilistic energy and operation management of a microgrid containing wind/photovoltaic/fuel cell generation and energy storage devices based on point estimate method and self-adaptive gravitational search algorithm. *Energy*, 43, 427–437.
- Orban, J., & Richardson, N.W. (1995). Method for directionally drilling a borehole. *US Patent US5467832*, Schlumberger Technology Corporation.
- Rafsanjani, M.K., & Dowlatshahi, M.B. (2012). Using gravitational search algorithm for finding near-optimal base station location in two-tiered WSNs. *International Journal of Machine Learning and Computing*, 2, 377–380.
- Rashedi, E., Nezamabadi-pour, H., & Saryazdi, S. (2009). GSA: A gravitational search algorithm. *Information Sciences*, 179, 2232–2248.
- Rashidi, B., Hareland, G., & Nygaard, R. (2008). *Real-time drill bit wear prediction by combining rock energy and drilling strength concepts*. Abu Dhabi International Petroleum Exhibition and Conference, Abu Dhabi, UAE.
- Rostamy, A.S., Bernety, H.M., & Hosseinabadi, A.R. (2011, Dec 27–29). A novel and optimized algorithm to select monitoring senses by GSA. *2nd International Conference on Control, Instrumentation and Automation* (pp. 829–834). Shiraz, Iran.
- Rubio-Largo, Á., Vega-Rodríguez, M., Gómez-Pulido, J., & Sánchez-Pérez, J. (2011). A multiobjective gravitational search algorithm applied to the static routing and wavelength assignment problem. In *Applications of evolutionary computation, EvoApplications 2011* (Vol. 6625, pp. 41–50). Springer Berlin Heidelberg.
- Sabri, N.M., Puteh, M., & Mahmood, M.R. (2013). An overview of Gravitational Search Algorithm utilization in optimization problems. *2013 IEEE 3rd International Conference on System Engineering and Technology (ICSET)* (pp. 61–66), 19–20 Aug., Shah Alam, Malaysia.
- Sun, G., Zhang, A., Yao, Y., & Wang, Z. (2016). A novel hybrid algorithm of gravitational search algorithm with genetic algorithm for multi-level thresholding. *Applied Soft Computing*, 46, 703–730.
- Talib, M., Elshafei, M., Khoukhi, A., Saif, A.W.A., & Abdulazeez, A. (2014). Modeling and control of quad-rotor Directional Steering System. *2014 IEEE International Symposium on Innovations in Intelligent Systems and Applications (INISTA) Proceedings*, 23–25 June. Alberobello, Italy.
- Tan, X., & Bhanu, B. (2006). Fingerprint matching by genetic algorithms. *Pattern Recognition*, 39, 465–477.
- Voos, H. (2009). Nonlinear control of a quadrotor micro-UAV using feedback-linearization. *2009 IEEE International Conference on Mechatronics, April*, 14–17 April, Malaga, Spain.
- Wenzel, K.H. (1988). Adjustable bent sub. *US Patent US4745982*, 4–7, Kenneth H. Wenzel Oilfield Consulting Inc., Edmonton, CA.
- Williams, E.B. (1956). Jetting device for rotary drilling apparatus. *US Patent US2765146*, Greenville, Texas.
- Wu, J., & Wisler, M.M. (1993). Method for drilling directional wells. *US Patents US5230386*, Baker Hughes Incorporated, Texas.
- Xue, Y., Zhong, S., Ma, T., & Cao, J. (2016). A hybrid evolutionary algorithm for numerical optimization problem. *Intelligent Automation & Soft Computing*, 8587(November), 21 (4), 473–490.
- Yiyong, Y.Y.Y., Baolin, L.B.L., Kai, Z.K.Z., Dianfeng, Z.D.Z., & Jian, C.J.C. (2009). Control unit of the directional drilling system. *Chinese Control and Decision Conference*, 2009, 1000–1004.